

Experimental Study of the BEC-BCS Crossover Region in Lithium 6

T. Bourdel, L. Khaykovich, J. Cubizolles, J. Zhang, F. Chevy, M. Teichmann, L. Tarruell,
S. J. J. M. F. Kokkelmans, and C. Salomon

Laboratoire Kastler-Brossel, ENS, 24 rue Lhomond, 75005 Paris

(Received 2 March 2004; revised manuscript received 14 April 2004; published 27 July 2004)

We report Bose-Einstein condensation of weakly bound ${}^6\text{Li}_2$ molecules in a crossed optical trap near a Feshbach resonance. We measure a molecule-molecule scattering length of 170_{-60}^{+100} nm at 770 G, in good agreement with theory. We study the 2D expansion of the cloud and show deviation from hydrodynamic behavior in the BEC-BCS crossover region.

DOI: 10.1103/PhysRevLett.93.050401

PACS numbers: 03.75.Ss, 05.30.Fk, 32.80.Pj, 34.50.-s

By applying a magnetic field to a gas of ultracold atoms, it is possible to tune the strength and the sign of the effective interaction between particles. This phenomenon, known as Feshbach resonance, offers in the case of fermions the unique possibility to study the crossover between situations governed by Bose-Einstein and Fermi-Dirac statistics. Indeed, when the scattering length a characterizing the 2-body interaction at low temperature is positive, the atoms are known to pair in a bound molecular state. When the temperature is low enough, these bosonic dimers can form a Bose-Einstein condensate (BEC) as observed very recently in ${}^{40}\text{K}$ [1] and ${}^6\text{Li}$ [2,3]. On the side of the resonance where a is negative, one expects the well-known Bardeen-Cooper-Schrieffer (BCS) model for superconductivity to be valid. However, this simple picture of a BEC phase on one side of the resonance and a BCS phase on the other is valid only for small atom density n . When $n|a|^3 \gtrsim 1$ the system enters a strongly interacting regime that represents a challenge for many-body theories [4–6] and that now begins to be accessible to experiments [7–9].

In this Letter, we report on Bose-Einstein condensation of ${}^6\text{Li}$ dimers in a crossed optical dipole trap and a study of the BEC-BCS crossover region. Unlike all previous observations of molecular BEC made in single beam dipole traps with very elongated geometries, our condensates are formed in nearly isotropic traps. Analyzing free expansions of pure condensates with up to 4×10^4 molecules, we measure the molecule-molecule scattering length $a_m = 170_{-60}^{+100}$ nm at a magnetic field of 770 G. This measurement is in good agreement with the value deduced from the resonance position [9] and the relation $a_m = 0.6 a$ of Ref. [10]. Combined with tight confinement, these large scattering lengths lead to a regime of strong interactions where the chemical potential μ is on the order of $k_B T_C$ where $T_C \approx 1.5 \mu\text{K}$ is the condensation temperature. As a consequence, we find an important modification of the thermal cloud time of flight expansion induced by the large condensate mean field. Moreover, the gas parameter $n_m a_m^3$ is no longer small but on the order of 0.3. In this regime, the validity of mean field theory becomes questionable [11–13]. We show, in particular,

that the anisotropy and gas energy released during expansion varies monotonically across the Feshbach resonance.

Our experimental setup has been described previously [14,15]. A gas of ${}^6\text{Li}$ atoms is prepared in the absolute ground state $|1/2, 1/2\rangle$ in a Nd-doped yttrium aluminum garnet crossed beam optical dipole trap. The horizontal beam (respectively vertical) propagates along x (y), has a maximum power of $P_o^h = 2$ W ($P_o^v = 3.3$ W) and a waist of $\sim 25 \mu\text{m}$ ($\sim 40 \mu\text{m}$). At full power, the ${}^6\text{Li}$ trap oscillation frequencies are $\omega_x/2\pi = 2.4(2)$, $\omega_y/2\pi = 5.0(3)$, and $\omega_z/2\pi = 5.5(4)$ kHz, as measured by parametric excitation, and the trap depth is $\sim 80 \mu\text{K}$. After sweeping the magnetic field B from 5 to 1060 G, we drive the Zeeman transition between $|1/2, 1/2\rangle$ and $|1/2, -1/2\rangle$ with a 76 MHz rf field to prepare a balanced mixture of the two states. As measured very recently [9], the Feshbach resonance between these two states is peaked at 822(3) G, and for $B = 1060$ G, $a = -167$ nm. After 100 ms the coherence between the two states is lost and plain evaporation provides $N_\uparrow = N_\downarrow = N_{\text{tot}}/2 = 1.5 \times 10^5$ atoms at $10 \mu\text{K} = 0.8 T_F$, where $k_B T_F = \hbar^2 k_F^2/2m = \hbar(3N_{\text{tot}}\omega_x\omega_y\omega_z)^{1/3} = \hbar\bar{\omega}(3N_{\text{tot}})^{1/3}$ is the Fermi energy. Lowering the intensity of the trapping laser to $0.1 P_0$, the Fermi gas is evaporatively cooled to temperatures T at or below $0.2 T_F$ and $N_{\text{tot}} \approx 7 \times 10^4$.

Then, sweeping the magnetic field to 770 G in 200 ms, the Feshbach resonance is slowly crossed. In this process atoms are reversibly transformed into cold molecules [14,16] near the BEC critical temperature as presented in Fig. 1(a). The onset of condensation is revealed by bimodal and anisotropic momentum distributions in time of flight expansions of the molecular gas. These images are recorded as follows. At a fixed magnetic field, the optical trap is first switched off. The cloud expands typically for 1 ms and then the magnetic field is increased by 100 G in 50 μs . This converts the molecules back into free atoms above resonance without releasing their binding energy [3]. Switching the field abruptly off in 10 μs , we detect free ${}^6\text{Li}$ atoms by light absorption near the D2 line. Using this method, expansion images are not altered by the adiabatic following of the molecular state to a

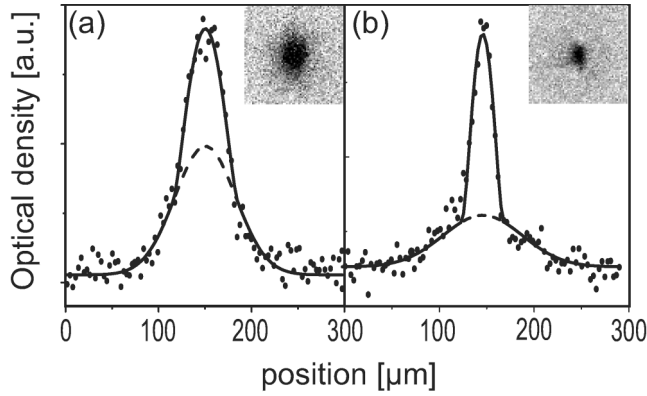


FIG. 1. Onset of Bose-Einstein condensation in a cloud of 2×10^4 ${}^6\text{Li}$ dimers at 770 G (a) and of 2×10^4 ${}^7\text{Li}$ atoms at 610 G (b) in the same optical trap. (a) 1.2 ms expansion profiles along the weak direction x of confinement. (b) 1.4 ms expansion. The different sizes of the condensates reflect the large difference in scattering length $a_m = 170$ nm for ${}^6\text{Li}$ dimers and $a_7 = 0.55$ nm for ${}^7\text{Li}$. Solid line: Gaussian+Thomas-Fermi fit. Dashed line: Gaussian component. Condensate fractions are both 28%. $\omega_x/2\pi = 0.59(4)$ kHz, $\omega_y/2\pi = 1.6(1)$ kHz, and $\omega_z/2\pi = 1.7(1)$ kHz in (a). $\omega_x/2\pi = 0.55(4)$ kHz, $\omega_y/2\pi = 1.5(1)$ kHz, and $\omega_z/2\pi = 1.6(1)$ kHz in (b).

deeper bound state during switch-off as observed in our previous work [14]. Furthermore, we check that there are no unpaired atoms before expansion. In Fig. 1(b), a Bose-Einstein condensate of ${}^7\text{Li}$ atoms produced in the same optical trap is presented. The comparison between the condensate sizes after expansion reveals that the mean field interaction and scattering length are much larger for ${}^6\text{Li}_2$ dimers [Fig. 1(a)] than for ${}^7\text{Li}$ atoms [Fig. 1(b)].

To measure the molecule-molecule scattering length, we produce pure molecular condensates by taking advantage of our crossed dipole trap. We recompress the horizontal beam to full power while keeping the vertical beam at the low power of $0.035P_0^y$ corresponding to a trap depth for molecules $U = 5.6 \mu\text{K}$. Temperature is then limited to $T \leq 0.9 \mu\text{K}$ assuming a conservative $\eta = U/k_B T = 6$, whereas the critical temperature increases with the mean oscillation frequency. Consequently, with an axial (respectively radial) trap frequency of 440 Hz (respectively 5 kHz), we obtain $T/T_C^0 \leq 0.3$, where $T_C^0 = \hbar\bar{\omega}(0.82N_{\text{tot}}/2)^{1/3} = 2.7 \mu\text{K}$ is the noninteracting BEC critical temperature. Thus, the condensate should be pure as confirmed by our images. After 1.2 ms of expansion, the radius of the condensate in the x (respectively y) direction is $R_x = 51 \mu\text{m}$ ($R_y = 103 \mu\text{m}$). The resulting anisotropy $R_y/R_x = 2.0(1)$ is consistent with the value 1.98 [17] predicted the scaling equations [18,19]. Moreover, this set of equations leads to an *in-trap* radius $R_x^0 = 26 \mu\text{m}$ (respectively $R_y^0 = 2.75 \mu\text{m}$). We then deduce the molecule-molecule scattering length from the Thomas-Fermi formula $R_{x,y}^0 =$

$a_{\text{ho}}\bar{\omega}/\omega_{x,y}(15N_{\text{tot}}a_m/2a_{\text{ho}})^{1/5}$, with $a_{\text{ho}} = \sqrt{\hbar/2m\bar{\omega}}$. Averaging over several images, this yields $a_m = 170_{-60}^{+100}$ nm at 770 G. Here, the statistical uncertainty is negligible compared to the systematic uncertainty due to the calibration of our atom number. At this field, we calculate an atomic scattering length of $a = 306$ nm. Combined with the prediction $a_m = 0.6a$ of [10], we obtain $a_m = 183$ nm in good agreement with our measurement. For ${}^7\text{Li}$, we obtain with the same analysis a much smaller scattering length of $a_7 = 0.65(10)$ nm at 610 G also in agreement with theory [20].

Such large values of a_m bring our molecular condensates into a novel regime where the gas parameter $n_m a_m^3$ is no longer very small. Indeed, $a_m = 170$ nm and $n_m = 6 \times 10^{13} \text{ cm}^{-3}$ yield $n_m a_m^3 = 0.3$. As a first consequence, corrections due to beyond mean field effects [11,21] or to the underlying fermionic nature of atoms may play a role, since the average spacing between molecules is then of the order of the molecule size $\sim a/2$. Second, even in a mean field approach, thermodynamics is expected to be modified. For instance, in the conditions of Fig. 1(a), we expect a large shift of the BEC critical temperature [11–13]. The shift calculated to first order in $n^{1/3}a$ [12], $\Delta T_C/T_C^0 = -1.4$, is clearly inapplicable and a more refined approach is required [22]. Third, we observe that partially condensed cloud expansions are modified by interactions. Indeed, double structure fits lead to temperatures inconsistent with the presence of a condensate. In Fig. 1, we find $T = 1.6 \mu\text{K}$, to be compared with $T_C^0 = 1.4 \mu\text{K}$, whereas for the ${}^7\text{Li}$ condensate $T = 0.7 \mu\text{K} = 0.6T_C^0$.

This inconsistency results from the large mean field interaction which modifies the thermal cloud expansion. To get a better estimate of the temperature, we rely on a release energy calculation. We calculate the Bose distribution of thermal atoms in a Mexican hat potential that is the sum of the external potential and the repulsive mean field potential created by the condensate. For simplicity we neglect the mean field resulting from the thermal component. The release energy is the sum of the thermal kinetic energy, condensate interaction energy, and Hartree-Fock interaction energy between the condensate and thermal cloud. The temperature and chemical potential are then adjusted to fit the measured atom number and release energy. For Fig. 1(a), we obtain a condensate fraction of 28% and $\mu = \hbar\bar{\omega}/2(15N_C a_m/2a_{\text{ho}})^{2/5} = 1.4 \mu\text{K}$. The temperature $T = 0.9 \mu\text{K}$ is then found below $T_C^0 = 1.4 \mu\text{K}$.

The condensate lifetime is typically ~ 300 ms at 715 G ($a_m = 66$ nm) and ~ 3 s at 770 G ($a_m = 170$ nm), whereas for $a = -167$ nm at 1060 G, the lifetime exceeds 30 s. On the BEC side, the molecule-molecule loss rate constant is $G = 0.26_{-0.06}^{+0.08} \times 10^{-13} \text{ cm}^3/\text{s}$ at 770 G and $G = 1.75_{-0.4}^{+0.5} \times 10^{-13} \text{ cm}^3/\text{s}$ at 715 G with the fit procedure for condensates described in [23]. Combining similar results for four values of the magnetic field ranging from 700 to 770 G, we find $G \propto a^{-1.9 \pm 0.8}$. Our data are in

agreement with the theoretical prediction $G \propto a^{-2.55}$ of Ref. [10] and with previous measurements of G in a thermal gas at 690 G [14] or in a BEC at 764 G [8]. A similar power law was also found for ^{40}K [24].

We now present an investigation of the crossover from a Bose-Einstein condensate to an interacting Fermi gas (Figs. 2 and 3). We prepare a nearly pure condensate with 3.5×10^4 molecules at 770 G and recompress the trap to frequencies of $\omega_x = 2\pi \times 830$ Hz, $\omega_y = 2\pi \times 2.4$ kHz, and $\omega_z = 2\pi \times 2.5$ kHz. The magnetic field is then slowly swept at a rate of 2 G/ms to various values across the Feshbach resonance. The 2D momentum distribution after a time of flight expansion of 1.4 ms is then detected as previously.

Figure 2 presents the observed profiles (integrated over the orthogonal direction) for different values of the magnetic field. At the lowest field values $B \leq 750$ G, $n_m a_m^3 \ll 1$, condensates number are relatively low because of the limited molecule lifetime. As B increases, the condensate width gradually increases towards the width of a non-interacting Fermi gas, and nothing dramatic happens on resonance. At the highest fields ($B \geq 925$ G), where $k_F |a| \leq 3$, distributions are best fitted with zero temperature Fermi profiles. More quantitatively, Fig. 3(b) presents both the gas energy released after expansion E_{rel} and the anisotropy η across resonance. These are calculated from Gaussian fits to the density after time of flight: $E_{\text{rel}} = m(2\sigma_y^2 + \sigma_x^2)/2\tau^2$ and $\eta = \sigma_y/\sigma_x$, where σ_i is the rms width along i , and τ is the time of flight [17]. On the BEC side at 730 G, the measured anisotropy is $\eta \sim 1.6(1)$, in agreement with the hydrodynamic prediction, 1.75. It then decreases monotonically to 1.1 at 1060 G on the BCS side. On resonance, at zero temperature, superfluid hydrodynamic expansion is expected [25] corresponding to $\eta = 1.7$. We find, however, $\eta = 1.35(5)$, indicating a

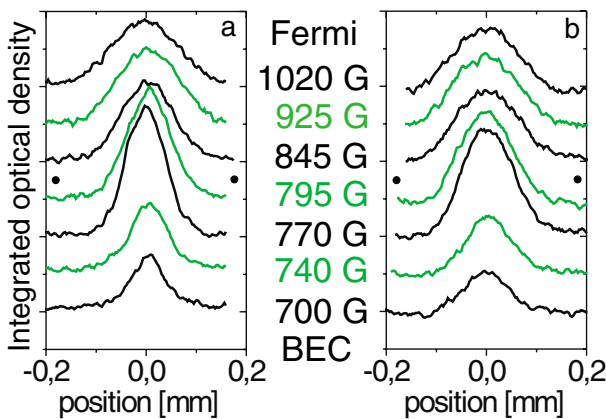


FIG. 2 (color online). Integrated density profiles across the BEC-BCS crossover region. 1.4 ms time of flight expansion in the axial (a) and radial (b) direction. The magnetic field is varied over the whole region of the Feshbach resonance from $a > 0$ ($B < 822$ G) to $a < 0$ ($B > 822$ G). ●: Feshbach resonance peak.

partially hydrodynamic behavior that could be due to a reduced superfluid fraction. On the $a < 0$ side, the decreasing anisotropy would indicate a further decrease of the superfluid fraction that could correspond to the reduction of the condensed fraction of fermionic atom pairs away from resonance observed in [7,9]. Interestingly, our results differ from that of Ref. [26] where hydrodynamic expansion was observed at 910 G in a more elongated trap for $T/T_F \approx 0.1$.

In the BEC-BCS crossover regime, the gas energy released after expansion E_{rel} is also smooth [Fig. 3(c)]. E_{rel} presents a plateau for $B \leq 750$ G, and then increases monotonically towards that of a weakly interacting Fermi

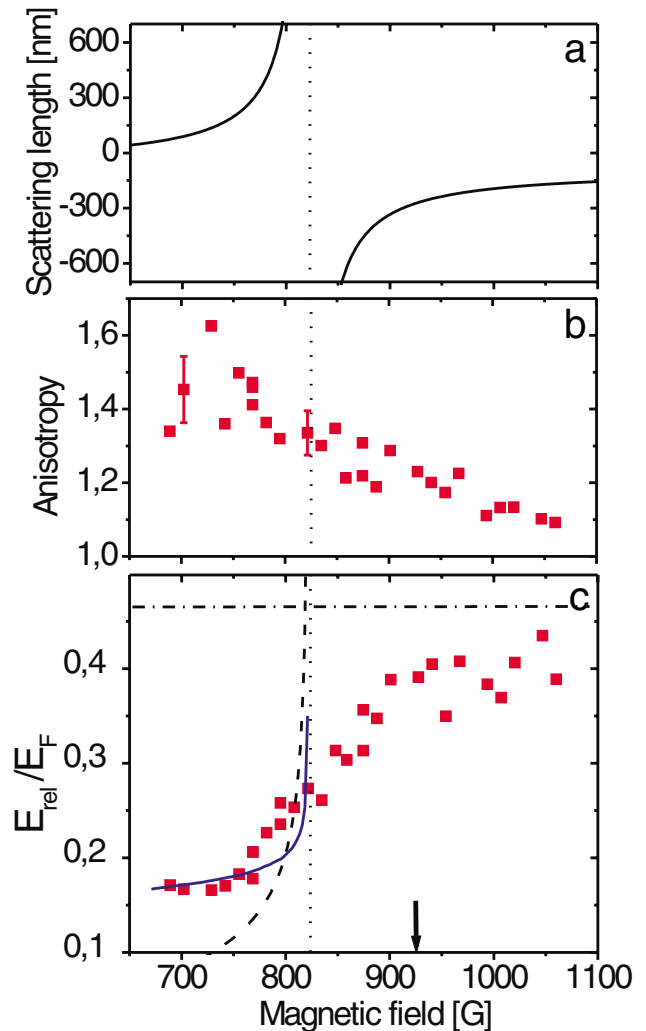


FIG. 3 (color online). (a) scattering length between the $|1/2, 1/2\rangle$ and $|1/2, -1/2\rangle$ ^6Li states. The Feshbach resonance peak is located at 822 G (dotted line). (b): anisotropy of the cloud, (c) release energy across the BEC-BCS crossover region. In (c), the dot-dashed line corresponds to a $T = 0$ ideal Fermi gas. The dashed curve is the release energy from a pure condensate in the Thomas-Fermi limit. The solid curve corresponds to a finite temperature mean field model described in the text with $T = 0.6 T_C^0$. Arrow: $k_F |a| = 3$.

gas. The plateau is not reproduced by the mean field approach of a pure condensate (dashed line). This is a signature that the gas is not at $T = 0$. It can be understood with the mean field approach we used previously to describe the behavior of the thermal cloud. Since the magnetic field sweep is slow compared to the gas collision rate [14], we assume that this sweep is adiabatic and conserves entropy [27]. We then adjust this entropy to reproduce the release energy at a particular magnetic field, $B = 720$ G. The resulting curve as a function of B (solid line in Fig. 3(c)) agrees well with our data in the range $680 \text{ G} \leq B \leq 770 \text{ G}$, where the condensate fraction is 40%, and the temperature is $T \approx 0.6T_C^0 = 1.4 \mu\text{K}$. This model is limited to $n_m a_m^3 \lesssim 1$. Near resonance the calculated release energy diverges and clearly departs from the data. On the BCS side, the release energy of a $T = 0$ ideal Fermi gas gives an upper bound for the data (dot-dashed curve), as expected from negative interaction energy and a very cold sample. This low temperature is supported by our measurements on the BEC side and the assumption of entropy conservation through resonance which predicts $T = 0.1 T_F$ [27].

On resonance the gas is expected to reach a universal behavior, as the scattering length a is not a relevant parameter any more [5]. In this regime, the release energy scales as $E_{\text{rel}} = \sqrt{1 + \beta E_{\text{rel}}^0}$, where E_{rel}^0 is the release energy of the noninteracting gas and β is a universal parameter. From our data at 820 G, we get $\beta = -0.64(15)$. This value is larger than the Duke result $\beta = -0.26 \pm 0.07$ at 910 G [26], but agrees with that of Innsbruck $\beta = -0.68_{-0.10}^{+0.13}$ at 850 G [8], and with the most recent theoretical prediction $\beta = -0.56$ [6]. Around 925 G, where $a = -270 \text{ nm}$ and $(k_F|a|)^{-1} = 0.35$, the release energy curve displays a change of slope. This is a signature of the transition between the strongly and weakly interacting regimes. It is also observed near the same field in [8] through *in situ* measurement of the trapped cloud size. Interestingly, the onset of resonance condensation of fermionic atom pairs observed in ^{40}K [7] and ^6Li [9], corresponds to a similar value of $k_F|a|$.

In summary, we have explored the whole region of the ^6Li Feshbach resonance, from a Bose-Einstein condensate of fermion dimers to an ultracold interacting Fermi gas. The extremely large scattering length between molecules that we have measured leads to novel BEC conditions. We have observed hydrodynamic expansions on the BEC side and nonhydrodynamic expansions at and above resonance. We suggest that this effect results from a reduction of the superfluid fraction and we point to the need of a better understanding of the dynamics of an expanding Fermi gas.

We are grateful to Y. Castin, C. Cohen-Tannoudji, R. Combescot, J. Dalibard, G. Shlyapnikov, and S. Stringari for fruitful discussions. This work was supported by CNRS, Collège de France, and Région Ile de France. S. Kokkelmans acknowledges a Marie Curie

grant from the E.U. under Contract No. MCFI-2002-00968. Laboratoire Kastler-Brossel is Unité de recherche de l'Ecole Normale Supérieure et de l'Université Pierre et Marie Curie, associée au CNRS.

-
- [1] M. Greiner, C. A. Regal, and D. S. Jin, *Nature (London)* **426**, 537 (2003).
 - [2] S. Jochim *et al.*, *Science* **302**, 2101 (2003).
 - [3] M. W. Zwierlein *et al.*, *Phys. Rev. Lett.* **91**, 250401 (2003).
 - [4] A. J. Leggett, *J. Phys. C (Paris)* **41**, 7 (1980); P. Nozières and S. Schmitt-Rink, *J. Low Temp. Phys.* **59**, 195 (1985); C. Sá de Melo, M. Randeria, and J. Engelbrecht, *Phys. Rev. Lett.* **71**, 3202 (1993); M. Holland, S. Kokkelmans, M. Chiofalo, and R. Walser, *Phys. Rev. Lett.* **87**, 120406 (2001); Y. Ohashi and A. Griffin, *Phys. Rev. Lett.* **89**, 130402 (2002); J. N. Milstein, S. J. J. M. F. Kokkelmans, and M. J. Holland, *Phys. Rev. A* **66**, 043604 (2002); R. Combescot, *Phys. Rev. Lett.* **91**, 120401 (2003); G. M. Falco and H. T. C. Stoof, *cond-mat/0402579*.
 - [5] H. Heiselberg, *Phys. Rev. A* **63**, 043606 (2001).
 - [6] J. Carlson, S.-Y. Chang, V. R. Pandharipande, and K. E. Schmidt, *Phys. Rev. Lett.* **91**, 050401 (2003).
 - [7] C. A. Regal, M. Greiner, and D. S. Jin, *Phys. Rev. Lett.* **92**, 040403 (2004).
 - [8] M. Bartenstein *et al.*, *Phys. Rev. Lett.* **92**, 120401 (2004).
 - [9] M. Zwierlein *et al.*, *Phys. Rev. Lett.* **92**, 120403 (2004).
 - [10] D. S. Petrov, C. Salomon, and G. V. Shlyapnikov, *cond-mat/0309010*.
 - [11] G. Baym *et al.*, *Eur. Phys. J. B* **24**, 107 (2001).
 - [12] F. Dalfovo, S. Giorgini, L. P. Pitaevskii, and S. Stringari, *Rev. Mod. Phys.* **71**, 463 (1999).
 - [13] F. Gerbier *et al.*, *Phys. Rev. Lett.* **92**, 030405 (2004).
 - [14] J. Cubizolles *et al.*, *Phys. Rev. Lett.* **91**, 240401 (2003).
 - [15] T. Bourdel *et al.*, *Phys. Rev. Lett.* **91**, 020402 (2003).
 - [16] C. A. Regal, C. Ticknor, J. L. Bohn, and D. S. Jin, *Nature (London)* **424**, 47 (2003).
 - [17] We correct our data for the presence of a magnetic field curvature which leads to an antitrapping frequency of 100 Hz at 800 G along x .
 - [18] Yu. Kagan, E. L. Surkov, and G. V. Shlyapnikov, *Phys. Rev. A* **54**, 1753(R) (1996).
 - [19] Y. Castin and R. Dum, *Phys. Rev. Lett.* **77**, 5315 (1996).
 - [20] L. Khaykovich *et al.*, *Science* **296**, 1290 (2002).
 - [21] L. Pitaevskii and S. Stringari, *Phys. Rev. Lett.* **81**, 4541 (1998).
 - [22] A mean field self-consistent calculation of the molecular density profile in the trap at T_C leads to $T_C^{\text{mf}} = 0.58T_C^0 \approx 0.8 \mu\text{K}$. S. Kokkelmans (to be published).
 - [23] J. Söding *et al.*, *Appl. Phys. B* **69**, 257 (1999).
 - [24] C. Regal, M. Greiner, and D. Jin, *Phys. Rev. Lett.* **92**, 083201 (2004).
 - [25] C. Menotti, P. Pedri, and S. Stringari, *Phys. Rev. Lett.* **89**, 250402 (2002).
 - [26] K. O'Hara *et al.*, *Science* **298**, 2179 (2002); M. Gehm *et al.*, *Phys. Rev. A* **68**, 011401 (2003).
 - [27] L. D. Carr, G. V. Shlyapnikov, and Y. Castin, *Phys. Rev. Lett.* **92**, 150404 (2004).